Intrinsic magnetism in $Zn_{1-x}Co_xO$ ($0.03 \leq x \leq 0.10$) thin films prepared by ultrasonic spray pyrolysis

2008 J. Phys.: Condens. Matter 20 315005

(http://iopscience.iop.org/0953-8984/20/31/315005)

J. Phys.: Condens. Matter **20** (2008) 315005 (6pp) doi:10.1088/0953-8984/20/31/315005

Intrinsic magnetism in $Zn_{1-x}Co_xO$ ($0.03 \leqslant x \leqslant 0.10$) thin films prepared by ultrasonic spray pyrolysis

Preetam Singh[1,3], Deepak[1], Rajendra N Goyal[2], Ashish K Pandey[2] and Davinder Kaur[1]

[1] Department of Physics and Center of Nanotechnology, Indian Institute of Technology Roorkee, Roorkee-247667, India
[2] Department of Chemistry and Center of Nanotechnology, Indian Institute of Technology Roorkee, Roorkee-247667, India

E-mail: preetamphy@gmail.com

Received 12 January 2008, in final form 6 May 2008
Published 26 June 2008
Online at stacks.iop.org/JPhysCM/20/315005

Abstract

The $Zn_{1-x}Co_xO$ thin films were prepared on a commercial glass substrate at 400 °C by ultrasonic spray pyrolysis. The effect of doping concentration on the structural, optical and magnetic properties of these films has been studied. The structural and optical properties of these films reflect the fact that the Co^{2+} ions have substituted the Zn^{2+} ions without changing the wurtzite structure of ZnO. We have not observed any secondary phases even after doping the 10 at.% concentration of Co. All the films were highly oriented with preferred (002) direction. By increasing the Co content, a systematic change in both the *c*-axis lattice constant and the fundamental band gap energy was observed. Three absorption bands were found in the transmission spectra of the Co doped ZnO films at 657 nm (1.89 eV), 610 nm (2.03 eV) and 567 nm (2.20 eV). The absorption bands were attributed to d–d intraionic transitions of tetrahedrally coordinated high-spin Co^{2+} ions. Magnetic studies reveal the absence of room temperature ferromagnetic behaviour in these films. The values of coercivity (H_C) $\sim$ 145 and 123 Oe and remanent magnetization (M_r) $\sim 4.32 \times 10^{-5}$ and 7.28 emu cm^{-2} were observed at 5 K for $Zn_{0.95}Co_{0.05}O$ and $Zn_{0.93}Co_{0.07}O$ thin films.

(Some figures in this article are in colour only in the electronic version)

1. Introduction

In recent years, extensive studies have been carried out to modify the properties of zinc oxide for different applications [1, 2]. Doping with transition metal elements leads to many interesting properties of ZnO. In 2000, Dietl *et al* [3] used a simple theory to estimate the T_c of ferromagnetic semiconductors, and they predicted that room temperature ferromagnetic semiconductors might be created by substituting cobalt ions in wide band gap semiconductors such as GaN and ZnO. Reports of ZnO-based room temperature ferromagnetic semiconductors [4] soon followed. Currently, much experimental and theoretical research is focused on dilute magnetic semiconductors (DMS) based on ZnO doped with transition metal ions such as Co, since the predicted room temperature ferromagnetism in DMS may be useful in spintronics [1]. The mechanism leading to room temperature ferromagnetism in Co doped ZnO is not fully established and there are many contradictory experimental observations. Even more startling are claims that undoped films of some of these oxides are ferromagnetic, or that they can become magnetic when doped with nonmagnetic cations. Examples are HfO_2 [5] and ZnO doped with Sc [6]. The term 'd^o ferromagnetism' has been suggested for these cases. Some research groups describe the observed FM ordering as an intrinsic effect [7, 8], while others describe it as an extrinsic effect [9–11] (due to the formation of Co clusters, the presence of Zn doped Co_3O_4 phase etc). Recently Bhatti *et al* have observed the room temperature ferromagnetism in a ZnO:Co sample (5 at.%) with

[3] Author to whom any correspondence should be addressed.

Table 1. Optimized spray parameters for $Zn_{1-x}Co_xO$ thin films.

Spray mode	Ultrasonic nebulizer
Air blast	Atomizer
Ultrasonic frequency (MHz)	1.7
Droplet size (μm)	2.8
Solution flow rate (ml h^{-1})	10
Distance from heater to substrate (cm)	5
Solvent	Distilled water and methanol
Precursor	Zinc nitrate and cobalt nitrate
Concentration (mol l^{-1})	0.1
Doping concentration (at.%)	3, 5, 7 and 10
Deposition temperature (°C)	400
Substrate	Glass

a Curie temperature ∼450 °C [11]. ZnCoO films obtained by the sol–gel method were found to be ferromagnetic with $T_c > 300$ K by Lee *et al* [12]. Although the presence of a secondary phase was noted in the samples $x > 0.25$. Films of Co doped ZnO prepared by pulsed laser deposition are reported to be ferromagnetic at room temperature [13], but Norton *et al* [14] suggest that Co nanocrystallites present in the sample could be responsible for ferromagnetism. These studies indicate that the magnetic properties of Co doped ZnO are highly sensitive to the preparation methods and conditions.

$Zn_{1-x}Co_xO$ ($0.03 \leqslant x \leqslant 0.10$) thin films were grown on commercial glass substrates by a simple and low cost ultrasonic spray pyrolysis technique. The spray pyrolysis technique has been adopted for the synthesis of Co doped ZnO thin films, because the process has many advantages such as better stoichiometry control, better homogeneity, low processing temperature, lower cost, easier fabrication of large area films, the possibility of using high-purity starting materials and having an easy coating process of large and complex-shaped substrates. Earlier we have reported the successful fabrication of pure nanocrystalline ZnO thin films and nanopowder by the same technique [15]. In the present study we have tried to investigate the effect of doping concentration on the structural, optical and magnetic properties of Co doped ZnO thin films.

2. Experimental details

The $Zn_{1-x}Co_xO$ thin films were prepared from aqueous solution of zinc nitrate [$Zn(NO_3)_2{\cdot}6H_2O$], and cobalt nitrate [$Co(NO_3)_2{\cdot}6H_2O$] dissolved in distilled water. For each doping concentration (x), a separate solution was made. The substrates were first ultrasonically degreased with acetone, ethanol and deionized water. Various parameters such as nozzle to substrate distance, deposition rate and flow rate of air (carrier gas), deposition temperature and concentration were optimized to get good quality films, as shown in table 1. A specially designed digital substrate heater with a temperature controller from Excel instruments was used to heat the substrate.

The rate of deposition was controlled by the carrier gas flow rate, substrate temperature as well as by precursor concentration. The films were deposited on a glass (component: $CaO{:}NaO{:}6SiO_2$) substrate at a fixed substrate temperature of 400 °C. The chemical solution was atomized into a stream of fine droplets via an ultrasonic nebulizer operated at an atomizing frequency of 1.7 MHz. The nitrate precursor solution was poured into the vessel from the inlet side. The aerosol was generated from the vibration of the transducer. The nebulized spray, which goes up in the column, was deposited on a hot substrate. The orientation and crystallinity of these thick films were studied using a Bruker AXS C-8 advanced diffractometer (1.54 Å) in θ–2θ geometry. A Perkin Elmer Lambda 25 UV–visible spectrometer was used to study the optical properties of films. Energy dispersive x-ray analysis (EDAX) was carried out on various samples by comparing the peaks and it confirms the concentrations of Co to be close to those in the stated composition. The film thickness was measured using a surface profilometer. The magnetic properties were investigated by a superconducting quantum interference device (SQUID) magnetometer (Quantum design, MPMS, XL).

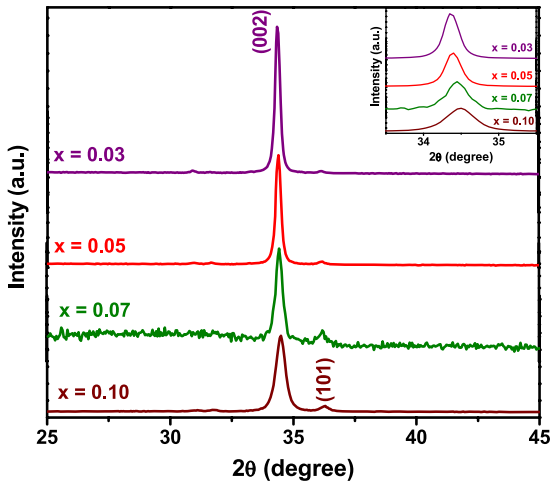

Figure 1. XRD pattern of the $Zn_{1-x}Co_xO$ ($x = 0.03$, 0.05, 0.07 and 0.10) thin film deposited on glass at 400 °C. The inset shows the broadening of the 002 peak.

3. Results and discussion

3.1. Structural properties

Figure 1 shows the x-ray diffraction patterns of the $Zn_{1-x}Co_xO$ ($x = 0.03$, 0.05, 0.07 and 0.10) thin films on glass substrate at 400 °C. All the films are shown single phase and have hexagonal wurtzite structure with the c-axis preferred orientation similar to our earlier reported results on pure ZnO thin films. ZnO usually grows along the (002) direction due to the lower surface free energy (1.6 J m^{-2}) of the (002) plane in comparison to the other (100) and (110) planes, which have surface free energies of 3.4 J m^{-2} and 2.0 J m^{-2} respectively [15]. No evidence of any other secondary phases and impurities (CoO, Co_3O_4 etc) were detected. The observation was attributed to the fact that the deposition temperature was relatively low to grow secondary phases such as CoO or Co_3O_4 in these films. Increasing cobalt concentration caused the slight shift in (002) peak position of these films to higher angles. Figure 2 shows the variation of

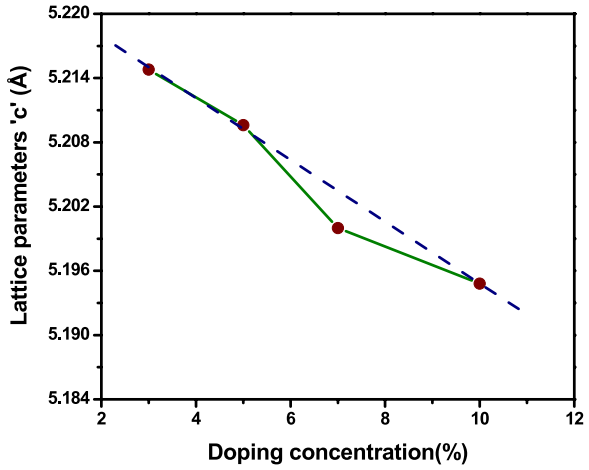

Figure 2. Variation of the c-axis lattice constant of $Zn_{1-x}Co_xO$ films for different Co concentration (x).

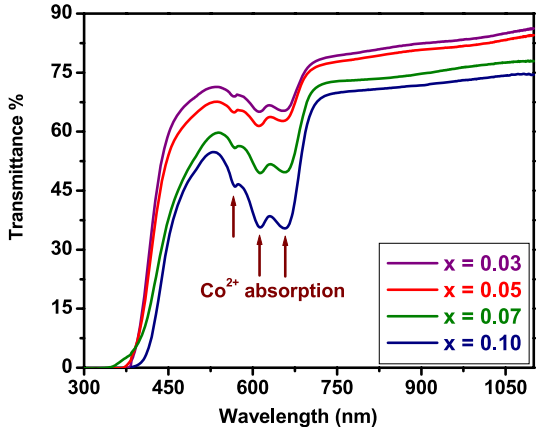

Figure 3. Transmission spectra of the $Zn_{1-x}Co_xO$ (with $x = 0.03$, 0.05, 0.07 and 0.10) thin films deposited on glass at 400 °C.

c-axis lattice constant of $Zn_{1-x}Co_xO$ films for different Co concentration (x). The value of the c-axis lattice constant was found to decrease from 5.2148 Å ($x = 0.03$), 5.2095 Å ($x = 0.05$), 5.200 Å ($x = 0.07$) to 5.1948 Å ($x = 0.10$). Similar dependence of the lattice constant on Co concentration is usually observed in the reported results on $Zn_{1-x}Co_xO$ films [16]. According to Vegard's law, this is quite expected for a Co substituted ZnO solid solution as the ionic radii of the Co^{2+} (0.72 Å) and Zn^{2+} (0.74 Å) in the tetrahedral coordination are nearly the same and as a result the unit cell parameters do not vary significantly with increase in doping concentration. Moreover, this also reflects that Co^{2+} ions were substituted by Zn^{2+} in ZnO without changing the wurtzite structure. A slight deviation observed in the c-axis parameter for $x = 0.07$ from Vegard's rule could be due to compensated defects [17]. The value of the peak width broadening of the $Zn_{1-x}Co_xO$ (002) peak was found to be increased with increase in the doping concentration of Co, indicating possible changes in the crystallite size and strain due to the Co^{2+} ion substitution. The observed increase in value of the FWHM of the (002) reflection was found to be 0.196 Å ($x = 0.03$), 0.201 Å ($x = 0.05$), 0.251 Å ($x = 0.07$) and 0.397 Å ($x = 0.10$) respectively. Further the crystallite size was calculated from XRD data and was observed to be 41.95 nm ($x = 0.03$), 40.90 nm ($x = 0.05$), 32.76 nm ($x = 0.07$) and 20.71 nm ($x = 0.10$) respectively. We have also calculated the grain size from atomic force microscopy (AFM) and field emission electron microscopy (FESEM) data (figures are not included in this paper), which was observed to be less than 100 nm in the case of all the films.

3.2. Optical properties

The optical transmission spectra of the $Zn_{1-x}Co_xO$ ($x = 0.03$, 0.05, 0.07 and 0.10) thin films deposited at 400 °C are shown in figure 3. The band edge of these films has been found to shift progressively towards lower energies with increase in doping concentration. This observed red shift with increasing Co concentration could be attributed to the sp–d exchange interactions between the band electrons and the localized d electrons of the Co^{2+} ions [18]. We believe that Co enters the tetrahedral sites of the wurtzite structure as Co^{2+} is seen as the transitions in the transmission spectra at 657 nm (1.89 eV), 610 nm (2.03 eV) and 567 nm (2.20 eV), assigned as d–d absorption levels of high-spin Co^{2+} ions in a tetragonal crystal field. They are assigned as $^4A_2(F) \rightarrow {}^2E(G)$, $^4A_2(F) \rightarrow {}^4T_1(P)$ and $^4A_2(F) \rightarrow {}^2A_1(G)$ transitions in high-spin state Co^{2+} (d^7) respectively. These absorptions were ascribed to charge transfer between donor and acceptor ionization levels located within the band gap of the ZnO host, and absorption band intensities are expected to be proportional to the Co^{2+} concentration in the ZnO thin film, provided the film thickness is the same. Taking this into account, the $Zn_{0.90}Co_{0.10}O$ film with highest Co concentration should exhibit the strongest absorption band, which was in confirmation with our results, as shown in figure 3. Optical absorption coefficient α was calculated from the following relation;

$$T = \frac{(1-R)^2 \exp(-\alpha t)}{1 - R^2 \exp(-2\alpha t)}$$

where R and T are the spectral reflectance and transmittance and t is the film thickness. For greater optical density ($\alpha t > 1$), the interference effects due to internal reflections as well as reflectance at normal incidence are negligible and the previous equation can be approximated as:

$$T \approx \exp(-\alpha t).$$

Optical absorption coefficient α is given by the approximate formula:

$$\alpha = -\frac{1}{t}\ln(T),$$

where t is the film thickness and T is the transmittance measured. The film thickness was measured using a surface profilometer. The thickness of all the films was almost 450 nm.

Absorption edges of semiconductors correspond to the threshold for charge transition between the highest nearly filled band and the lowest nearly empty band. According to inter-band absorption theory, the optical band of the films can be

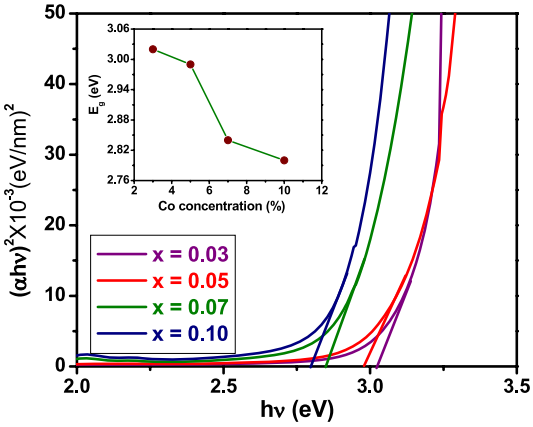

Figure 4. $(\alpha h\nu)^2$ versus $h\nu$ plots of $Zn_{1-x}Co_xO$ (with $x = 0.03$, 0.05, 0.07 and 0.10) thin films deposited on glass at 400 °C. The inset shows the variation of band gap with Co (%).

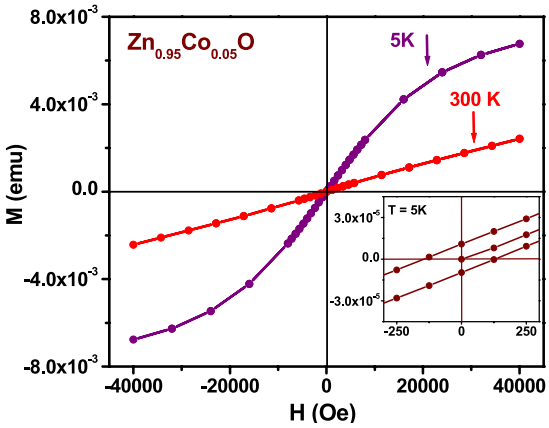

Figure 5. Magnetization versus magnetic field of $Zn_{0.95}Co_{0.05}O$ at 5 and 300 K of the films deposited at 400 °C. The inset shows the data for the low-field regions at 5 K.

calculated using the following relation [15]

$$\alpha h\nu = A(h\nu - E_g)^n$$

where A is the probability parameter for the transition, E_g is the band gap of the material, $h\nu$ is the incident photon energy, and n is the transition coefficient. The reported value of n is 2 for the measurement of an indirect band gap and 1/2 for a direct band gap. Figure 4 shows the plot of $(\alpha h\nu)^2$ against the photon energy $(h\nu)$ of the $Zn_{1-x}Co_xO$ ($x = 0.03$, 0.05, 0.07 and 0.10) thin films. The direct band gap of these films was determined by taking the intersection of the extrapolated lines from the linear vertical and horizontal regions near the band edge of the $(\alpha h\nu)^2 = 0$ curve. The calculated value of the band gap was 3.02, 2.99, 2.84 and 2.80 eV corresponding to $x = 0.03$, 0.05, 0.07 and 0.10 respectively in $Zn_{1-x}Co_xO$ thin films. The red shift of the absorption edge with increasing Co concentration is interpreted as mainly due to the sp–d exchange interactions between the band electrons and the localized d electrons of the Co^{2+} ions substituting Zn^{2+} ions and is inconsistent with the reported results [18]. The variation of energy band gap with increasing Co concentration from 3 to 10 at.% is shown in figure 4.

3.3. Magnetic properties

The magnetic properties of $Zn_{1-x}Co_xO$ (with $0.03 \leqslant x \leqslant 0.10$) thin films were carried out using a SQUID magnetometer. The area of the substrates used for the film deposition was 0.5×0.5 cm^2. The M–H curve of the $Zn_{0.95}Co_{0.05}O$ and $Zn_{0.93}Co_{0.07}O$ films at 5 and 300 K is shown in figures 5 and 6. The data have been corrected for the diamagnetic contribution due to the background signal from the glass substrate using equation $M_{film}(H) = M_{total}(H) - \chi_{substrate}.H$, where $\chi_{substrate}$ is the susceptibility of the substrate. We have not observed any prominent nonlinear hysteresis loop in the M–H curve. However, at 5 K, M versus H behaviour was nonlinear and the inset of figure 5 shows the low-field region of the loop, showing coercivity (H_C) of ∼145 Oe and remanent magnetization of about (M_r) ∼ 4.32×10^{-5} emu cm^{-2} for 5 at.% Co doped

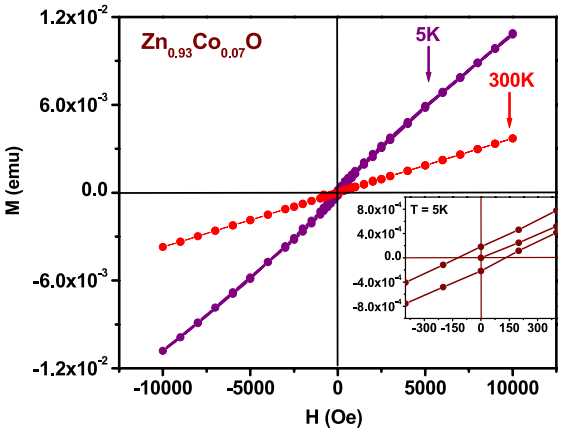

Figure 6. Magnetization versus magnetic field of $Zn_{0.93}Co_{0.07}O$ at 5 and 300 K for the films deposited at 400 °C. The inset shows the data for the low-field regions at 5 K.

ZnO film. However, 7 at.% Co doped ZnO film indicates H_C ∼ 123 Oe and M_r ∼ 7.28×10^{-4} emu cm^{-2}, as shown in the inset of figure 6. The low value of coercivity (<100 Oe) and high ordering temperatures (250–300 K) have been shown by Theodoropoulou *et al* in their Co and Mn implanted ZnO crystals [19]. To see the influence of deposition temperature on the magnetic properties of $Zn_{1-x}Co_xO$ films SQUID measurements were carried out on $Zn_{0.95}Co_{0.05}O$ thin films deposited at substrate temperatures of 500 °C. The M–H curve of the film at 5 K is shown in figure 7, which does not show any prominent nonlinear hysteresis loop.

The reported experimental results on the magnetic properties of Co doped ZnO are very different in thin films as well as in the bulk system. Earlier reported work on Co doped ZnO thin films showed them to be ferromagnetic with $T_C >$ 280 K [4]. However, there is a lot of discrepancy in the recently reported results. $Zn_{1-x}Co_xO$ films obtained by the sol–gel method were found to be ferromagnetic with $T_C > 300$ K [12], with the presence of a secondary phase. Films of Co doped ZnO prepared by pulsed laser deposition are reported to be ferromagnetic at room temperature [13], but Norton *et al* [14]

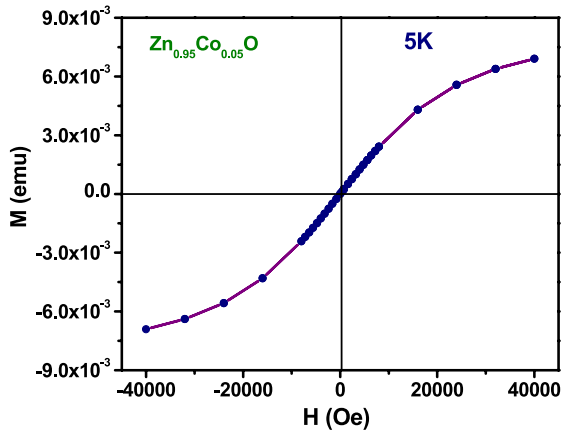

Figure 7. Magnetization versus magnetic field of $Zn_{0.95}Co_{0.05}O$ at 5 K for the film deposited at 500 °C.

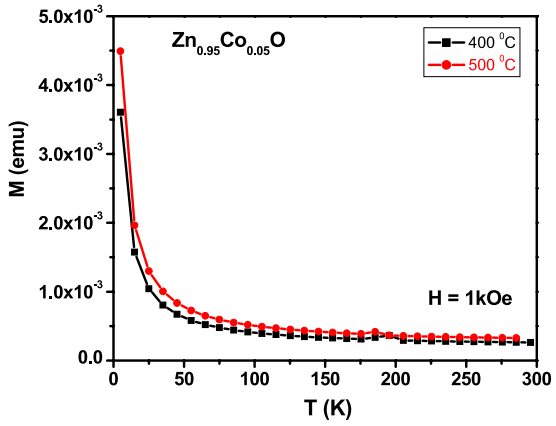

Figure 8. Temperature dependence of the magnetization curve at a field of 1 kOe for the $Zn_{0.95}Co_{0.05}O$ film deposited at 400 and 500 °C.

suggest that Co nanocrystallites present in the sample could be responsible for ferromagnetism. Risbud *et al* [20] show that well characterized stoichiometric bulk samples of $Zn_{1-x}Co_xO$ are not ferromagnetic and indicate dominant nearest-neighbour antiferromagnetic interaction. These samples were prepared by heating a solid solution of zinc and cobalt oxalates at a temperature of 1173 K for 15 min. From the reported results it was observed that where ferromagnetism has been found, the samples were heated to relatively high temperatures, which could give rise to spinel impurity phases. Risbud *et al*, however, report the absence of ferromagnetism in samples prepared at high temperatures. Even where the temperature of synthesis is relatively low, some of the synthesis procedures are not convincing as to whether the dopant has substituted the Zn site. While it is possible that Co clusters may be present in some of the Co–ZnO samples due to the reduction of Co^{2+} (that can occur in solution phase even at low temperatures), the presence of the magnetic spinel phases cannot be entirely eliminated in some of the preparations. Furthermore, the magnetization values reported by many workers are very low and can arise from the presence of magnetic impurities which cannot be detected by XRD.

Figure 8 shows the temperature dependence of magnetization of the $Zn_{0.95}Co_{0.05}O$ thin film deposited at substrate temperatures of 400 °C and 500 °C respectively, measured at a constant magnetic field of 1 kOe in the temperature range 5–300 K. Figure 9 shows the temperature dependence of $Zn_{0.93}Co_{0.07}O$ film deposited at 400 °C and measured at similar value of magnetic field and temperature range. In all these films it was observed that the magnetization changes slowly with decreasing temperature from 300 to 50 K, and afterwards there was a steep rise in magnetization below 50 K, showing the concave nature in the M–T curve at lower temperature, which can be explained by the polaron-percolation-theory reported by Das Sarma *et al* [21]. They have shown that the problem of ferromagnetic transition in a system of magnetic polarons is equivalent to the problem of overlapping spheres studied in percolation theory. In a system of magnetic polarons this condition satisfies ferromagnetic ordering with a highly concave nature in the M–T curve at lower temperatures. This generally happens in the case of a strongly localized insulating DMS. The

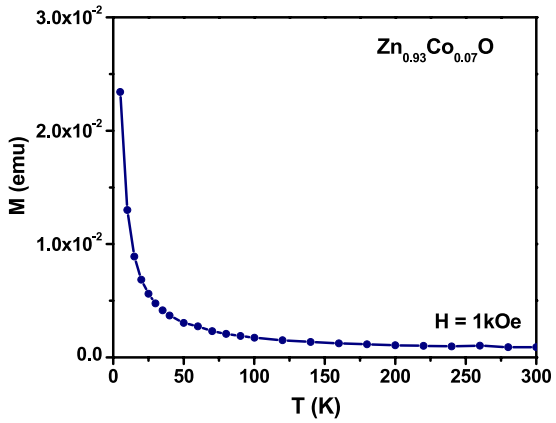

Figure 9. Temperature dependence of the magnetization curve at a field of 1 kOe for $Zn_{0.93}Co_{0.07}O$ film deposited at 400 °C.

effective radius of the polaron increases logarithmically with inverse temperature. At a very low temperature the effective radii of polarons are comparable to the size of the samples i.e. the formation of an infinite cluster corresponds the long range ordering of the ferromagnetic regime when many spins of magnetic impurity are polarized by the kinetic exchange interaction of the hole spin. Moreover, at low enough temperatures the neighbouring polarons are overlapped and the spins of polarons are aligned by the interaction of polarons through the magnetic impurities between them. In the presence of a disorder state, various types of spin-glass ground state may compete with the ferromagnetic ground state [22]. A first principles study has also shown that Co doped ZnO prefers to be in a spin glass state due to an antiferromagnetic super exchange interaction [23]. There have been several reports on measurements in different TM doped DMS thin films which have observed a concave nature in the M–T curve with steep rise of magnetization at lower temperatures without any magnetic transition down to the lowest attainable temperature [24]. However, there exists a prominent nonlinear hysteresis loop in the M–H curve for all those transition metal doped DMS thin films at lower temperatures. In our case of Co doped ZnO thin films, we have

observed a concave nature in the M–T curve with steep rise of magnetization at lower temperature, but we have not observed any prominent nonlinear hysteresis loop in the M–H curve.

In our case of $Zn_{1-x}Co_xO$ thin films synthesized by the spray pyrolysis technique, the constituent elements were mixed at molecular level, ensuring dopant atoms are present at substitutional sites as confirmed from XRD and optical properties of these films. Moreover, the deposition temperature was kept relatively low to avoid any possible impurity phase segregation even in relatively higher doping content. The absence of room temperature ferromagnetism in these films could possibly be due to neighbouring antiferromagnetic interactions, which suppress the ferromagnetic coupling, or due to the lack of free carriers in these films, which is in confirmation with the reports of Spaldin [25], which showed that robust ferromagnetism cannot occur in Mn and Co doped ZnO. If at all, it may occur if additional charge carriers are present.

4. Conclusions

In conclusion, we have successfully prepared $Zn_{1-x}Co_xO$ thin films with different doping concentration ($x = 0.03$, 0.05, 0.07 and 0.10) by ultrasonic spray pyrolysis at 400 °C. The structural and optical properties of these films reflect the fact that the Co^{2+} ions have substituted the Zn^{2+} ions without changing the wurtzite structure of ZnO. The observed decrease in band gap with increase in doping concentration of Co doped ZnO films was explained in terms of an sp–d exchange interaction. The concave nature of the M–T behaviour with steep rise of magnetization was observed at low temperature and was explained in terms of polaron-percolation-theory. Nonlinear behaviour of the magnetic moment was observed at both 5 K and 300 K. The value of coercivity $H_C \sim 123$ Oe and the remanent magnetization $M_r = 7.28 \times 10^{-4}$ emu cm^{-2} was observed at 5 K for 7 at.% Co doped ZnO thin films. We have not observed any secondary phases of cobalt oxides (CoO, Co_3O_4 etc) in the XRD curve, even after doping the 10 at.% of Co in these doped ZnO thin films. Thus the observed ferromagnetic ordering is due either to an intrinsic nature or because of defects. We have not observed room temperature ferromagnetism in $Zn_{1-x}Co_xO$ thin films.

Acknowledgments

The financial support provided by DST, India under the scheme Nanoscience and Technology Initiatives (NSTI) with reference No. DST SR/S5/NM-32/2005 and by the Ministry of Communications and Information Technology (MIT) under Nanotechnology initiatives division with reference No. 20(11)/2007-VCND is acknowledged. The author Preetam Singh is thankful to CSIR for the award of a senior research fellowship.

References

[1] Pearton S J, Abernathy C R, Overberg M E, Thaler G T, Norton D P, Theodoropoulou N, Hebard A F, Ren F, Kim J and Boatner L A 2003 *J. Appl. Phys.* **93** 1
[2] Pearton S J, Norton D P, Ip K, Heo Y W and Steiner T 2003 *Superlatt. Microstruct.* **34** 3
[3] Dietl T, Ohno H, Matsukura F, Cibert J and Ferrand D 2000 *Science* **287** 1019
[4] Ueda K, Tabata H and Kawai T 2001 *Appl. Phys. Lett.* **79** 988
[5] Hong N H, Sakai J, Poirot N and Brize V 2006 *Phys. Rev.* B **73** 132404
[6] Venkatesan M, Fitzgerald C B, Lunney J G and Coey J M D 2004 *Phys. Rev. Lett.* **93** 177206
[7] Schwartz D A, Norberg N S, Nguyen Q P, Parker J M and Gamelin D R 2003 *J. Am. Chem. Soc.* **125** 13205
[8] Sati P, Hayn R, Kuzian R, Regnier S, Schafer S, Stepanov A, Morhain C, Deparis C, Laugt M, Goiran M and Golacki Z 2006 *Phys. Rev. Lett.* **96** 017203
[9] Bhatti K P, Chaudhary S, Pandya D K and Kashyap S C 2006 *Solid State Commun.* **140** 23
[10] Jeong B S, Heo Y W, Norton D P, Kelly J G, Rairigh R, Hebard A F, Budai J D and Park Y D 2004 *Appl. Phys. Lett.* **84** 2608
[11] Bhatti K P, Chaudhary S, Pandya D K and Kashyap S C 2007 *J. Appl. Phys.* **101** 103919
[12] Lee H J, Jeong S Y, Cho C R and Park C H 2002 *Appl. Phys. Lett.* **81** 4020
[13] Ramachandran S, Tiwari A and Narayan J 2004 *Appl. Phys. Lett.* **84** 5255
[14] Norton D P, Overberg M E, Pearton S J, Pruessner K, Budai J D, Boatner L A, Chisolm M F, Lee J S, Khim Z G, Park Y D and Wilson R G 2003 *Appl. Phys. Lett.* **83** 5488
[15] Singh P, Kumar A, Deepak and Kaur D 2007 *J. Cryst. Growth* **306** 303
[16] Yan L and Ong C K 2004 *J. Appl. Phys.* **96** 1
[17] Ghosh R and Basak D 2007 *J. Appl. Phys.* **101** 023507
[18] Bhat V S and Deepak F L 2005 *Solid State Commun.* **135** 345
[19] Theodoropoulou N A, Hebard A F, Norton D P, Budai J D, Boatner L A, Lee J S, Khim Z G, Park Y D, Overberg M E, Pearton S J and Wilson R G 2003 *Solid-State Electron.* **47** 2231
[20] Risbud A S, Spaldin N A, Chen Z Q, Stemmer S and Seshadri R 2003 *Phys. Rev.* B **68** 205202
[21] Sarma S D, Hwang E H and Kaminski A 2003 *Phys. Rev.* B **67** 155201
[22] Timm C, Schafer F and Oppen F V 2002 *Phys. Rev. Lett.* **89** 137201
[23] Lee E C and Chang K J 2004 *Phys. Rev.* B **69** 85205-1
[24] Gu Z B, Yuan C S, Lu M H, Wang J, Wu D, Zhang S T, Zhu S N, Zhu Y Y and Chen Y F 2005 *J. Appl. Phys.* **98** 053908
[25] Spaldin N A 2004 *Phys. Rev.* B **69** 125201-1